Microsimulation Based Corrections on the Road Traffic Noise Emission Near Intersections

Bert De Coensel, Dick Botteldooren
Acoustics Group, Department of Information Technology, Ghent University, St. Pietersnieuwstraat 41, B-9000 Ghent, Belgium. bert.decoensel@intec.UGent.be

Filip Vanhove, Steven Logghe
Transport & Mobility Leuven, Vital Decosterstraat 67A, B-3000 Leuven, Belgium

Summary
Urban noise mapping traditionally involves the use of a traffic simulation model, which is often based on the estimation of macroscopic traffic flows. However, intersections and other local traffic management measures are not always modeled correctly. It is well known that the specific deceleration and acceleration dynamics of traffic at junctions can influence local noise emission. Finding the best strategy for using traffic modeling results in noise mapping is a current topic of research in the IMAGINE project. In this paper, a case study is presented, consisting of a large set of microscopic traffic simulations and associated noise emission calculations, which provides some insight into the specific dynamics of the noise emission near different types of intersections. It will be shown that it is possible to refine current traffic noise prediction models, based on macroscopic traffic simulation, using a correction on the average vehicle emission, aggregated in lane segments. A spatial approach should be used, in which inbound and outbound lanes are divided into deceleration, queuing, stopline and acceleration zones. Results from regression analysis on the numerical simulations indicate that meaningful relations between noise corrections and traffic flow parameters such as traffic intensity and composition can be deduced.

PACS no. 43.28.Hr, 43.50.Lj, 43.50.Rq

1. Introduction

Several national standards exist for the prediction of road traffic noise (for a review, see e.g. [1]). Most of these engineering models assume that roads can be divided into sections of considerable length where the vehicle flow can be considered homogeneous. Traffic flow calculations are usually based on traffic simulation models which consider average flow parameters. Traditionally, the sound emission caused by the traffic on each segment is modeled as a function mainly of the average vehicle speed and the traffic flow rate; most modern engineering models differentiate between the emissions produced by different types of vehicles [2].

However, the assumption of a spatially homogeneous traffic flow does not hold in the vicinity of junctions and other types of traffic delaying structures such as speed bumps; segments of constant noise emission have to be made smaller. In addition, average vehicle speeds calculated by macroscopic traffic simulation models become unreliable. For example, in the case of a signalized junction, a fraction of the traffic has to slow down to a halt, while another fraction of the traffic can cross the intersection without slowing down considerably. Finally, noise emission of stop-and-go traffic depends highly on vehicle acceleration, a parameter which can often not be reported by traditional traffic flow simulation models.

Because of these complications, the influence of intersections, and more in general of interrupted traffic flows, is evaluated mostly in a pragmatic way. The French prediction model, consisting of the Guide du Bruit [3] and the NMPB-96 propagation method [4], the UK CRTN prediction method [5] and the Swiss SonRoad road traffic noise model [6] do not include the impact of intersections at all – although recently efforts were undertaken to update the French model for different driving conditions [7]. In the Nordic model [8, 9], the use of a correction on the vehicle noise emission for continuous acceleration (after a crossing) and continuous deceleration (before a crossing) is proposed; however no input data for these driving conditions is available, and the model thus recommends to use only the cruising vehicle emission values. The Dutch RMW2002 model [10] includes an immission correction for intersections, depending on the intersection type and the diurnal traffic intensity. This correction can be at most 2.4 dB(A) at the center of the intersection and decreases linearly with the distance, for up to a distance of 150 m. The German RLS90 model [11] also includes an immis-

Received 21 June 2006,
accepted 14 December 2006.

sion correction term for intersections with traffic lights, for up to a distance of 100 m from the intersection. The non-European models of the US [12] and Japan [13, 14] both introduce a correction on the noise emission for transient driving conditions near intersections.

In spite of the fact that intersection corrections are only marginally taken into account in most prediction models in use today, there has been a reasonably amount of research on the topic of noise (reduction) from traffic management in the last three decades; a review can be found in [15]. In the UK, the earliest studies on interrupted traffic flows focused on L_{10} measurements nearby conventional intersections [16] and roundabouts [17, 18]. In general it was found that the noise from the accelerating traffic streams was within 1 dB(A) of the free flow level. In the early 1980's, basic computer models were introduced to predict traffic noise. In [19, 20, 21, 22], simulation models for L_{A10} for various types of interrupted flows were introduced. In a French study [23], a computer model for determining the noise radiated by a single vehicle approaching traffic lights was demonstrated. A Dutch model was also published [24], which was able to predict percentile noise levels of interrupted traffic flows in built-up environment. The propagation part for this model was based on transfer functions measured in a scale model. By the same author, a method for measuring the decrease and increase of vehicle noise levels at intersections was published [25].

After a less fruitful period, the study of noise at intersections gained renewed interest in the second half of the 1990's, possibly driven by new advances in the field of traffic modeling and the introduction of microsimulation models in traffic flow prediction. The STRADABruit model [26], developed by the French National Institute for Transport and Safety Research (INRETS), is based on a fluid dynamics macroscopic traffic model, modified to be able to represent transitional flow states at intersections, and coupled with a vehicle emission model based on test track measurements. This model was validated with measurements at a signalized intersection [27], and has recently been extended with a microsimulation model for special types of vehicles, and a more advanced propagation model [28]. Oshino *et al.* [29] made a coupling between a simple microsimulation model and a noise emission model for individual vehicles; a validation with measurements near various types of signalized intersections was also published [30, 31]. In the most recent models, a microsimulation model is coupled with an individual vehicle noise emission model and an advanced propagation model. The model developed at the University of Oviedo [32, 33], as well as the models developed at the University of Leeds [34, 35, 36] and at Ghent University [37, 38], make it possible to assess (percentile) traffic noise levels at (signalized) intersections in complex urban built-up environments. These models were recently updated for the latest Harmonoise vehicle noise emission model [39].

Measurements of the influence of the replacement of traffic lights by roundabouts on noise levels are discussed in [40], and a regression model for assessing their impact is deduced. It is found that, in ideal conditions, a reduction in $L_{Aeq,24h}$ of 1 to 4 dB can be achieved. A semi-analytical method to assess the noise impact of a roundabout is proposed in [41]; measurements are used to predict the kinematic parameters of vehicles traveling on the roundabout. In [42], road traffic noise was measured before and after the installation of traffic lights. In general, higher levels were found in the vicinity of the intersection, while lower levels were found at some distance from the lights. The last decade, there was also a more theoretical movement in traffic intersection noise research. In [43], a formula for the noise emitted from vehicles at a roundabout is derived analytically. A comprehensive number of analytical studies were performed by Kokowski and Makarewicz [44, 45, 46, 47], on the noise emitted from vehicles at signalized intersections and roundabouts.

Traffic noise prediction models that aim to be accurate in the vicinity of interrupted traffic flows, will have to model the temporal and spatial evolutions of vehicle speeds and accelerations. Microsimulation models can incorporate these dynamic effects. In recent efforts to harmonize traffic noise prediction on a European level [48], microsimulation models therefore are included. However, the main difficulties associated with microsimulation modeling are the large amount of detailed data on traffic flows needed and the fact that constructing and calibrating the model is time-consuming and only feasible for small to medium sized regions. When traffic noise prediction is based on a traffic model that does not simulate the dynamics of intersections, a correction could be applied to incorporate the effects on noise emissions.

In this article, a possible method to derive such corrections will be described, based on microsimulation results. Since it is not possible to simulate all conceivable intersection configurations and scenarios, a number of simple intersection scenarios were considered, in which a limited number of parameters were varied. This limits the applicability of the results described in this paper. However, in a typical real life study area, the variation in intersection types will not be very large, so the methodology desribed in this paper can easily be used to study the typical intersections in the study region, and to extrapolate the results to the whole network under study. In section 2, the general methodology will be described; section 3 discusses some insights gained into the specific dynamics of the noise immission near different types of intersections. Finally, intersection corrections that can be applied in case no microsimulation is available will be derived in section 4. A spatial approach will be used, in which inbound and outbound lanes are divided into deceleration, queuing, stopline and acceleration zones.

2. Methodology

2.1. Microsimulation models

To gain insight into the specific dynamics of the noise emission near different types of traffic junctions, a number of microscopic traffic simulation models were con-

structed. All models consisted of an intersection of a major road (inbound traffic flow of D_M vehicles·h^{-1}) and a minor road (inbound traffic flow of D_m vehicles·h^{-1}). A schematic view can be found in Figure 1. Both the major road and the minor road only have one lane in each direction, and the speed is limited to 70 km·h^{-1} on both roads. Four different intersection types (I) were considered: an intersection with a *priority-to-the-right* rule; an intersection where the major road has *priority*; an intersection with *traffic lights* and a *roundabout*.

By varying the traffic demands on the major and minor roads, different scenarios with calm, normal and busy traffic were created; six combinations were chosen (data can be found in Table I). Three variations in traffic composition, with a percentage F of heavy vehicles equal to 5 %, 10 % or 20 %, were considered. The number of scenarios was further increased by taking into account the percentage of the traffic that turns left or right (turning rate R), as this parameter may also influence congestion on certain types of intersections. Two situations were considered: one with 20 % turning traffic on both major and minor roads (10 % to the left and 10 % to the right), and one with 40 % turning traffic (20 % to the left and 20 % to the right). The total number of unique traffic scenarios is then equal to $\#I \times \#(D_M, D_m) \times \#F \times \#R = 4 \times 6 \times 3 \times 2 = 144$.

The microsimulation model parameters, such as the aggression, awareness and reaction time distribution of the vehicle drivers, the queue gap distance, the mean target headway between a vehicle and a following vehicle, the signposting distance etc., were not varied in this case study; standard values were used. Although these parameters have a significant influence on traffic dynamics near intersections, it is assumed that they do not vary much within a case study network. These parameters will have to be adjusted for the specific case study situation to which the methodology described in this paper is applied.

Road capacity and traffic light calibration was done on the basis of the Highway Capacity Manual [49]. Table I gives an overview of the traffic light timings for the signalized junction, which depend on the traffic flow and the turning rate. Quadstone Paramics [50] was chosen as the microsimulation model. The simulation time considered was 1 hour with a simulation timestep of $\Delta t = 0.5$ s. However, the actual simulations were run over 1 hour and 30 minutes, including an additional 10-minute period before the actual simulation for traffic build up, and a 20-minute period after the simulation for travel time calculations (see below). Traffic is loaded onto the network in zones at the ends of each arm of the intersection, at about 3 km from the center of the intersection, and randomly distributed in time. This distance makes it possible for the vehicles to arrive at the intersection with a more realistic temporal structure, consisting of groups of vehicles instead of purely random in time.

Due to the statistical nature of microsimulation, results differ between runs of the simulation. The simulated traffic flow, traffic composition, and turning rate will in each particular simulation run be near the demanded values, but will never meet them exactly. This reflects real situations, where the same average demand results in different situations from day to day. Since noise mapping reflects average situations, we are nevertheless mainly interested in average flows, speeds, queue lengths, etc. For each unique scenario, results were therefore averaged over 5 simulation runs with different seed values, to enable statistically sound conclusions. Average actual scenario traffic flows Q_M and Q_m and average percentages of heavy traffic F were extracted from the simulation runs, for each lane separately, using a dedicated Paramics plugin. These values may differ from the nominal values described in the previous section (which were used as model input parameters). However, the differences are only substantial for the traffic flows in the case of congestion (emphasized by a different notation for demand and flow); in this case the actual traffic flow Q_x will be less than the traffic demand D_x put forward. Nominal values of D_x, F and R will be used to simplify the discussion in section 3; the averaged values of Q_x and F, extracted from the actual simulations, will be used when deriving corrections in section 4.

Table I. Calibrated phase times for the signalized intersection, as a function of turning rate and traffic demand. The total signalization period consists of the indicated green time for the major arm plus 3 seconds of red time for both arms, and this repeated for the minor arm.

Turning rate R	Traffic demand [vehicles·h^{-1}] D_M–D_m	Allowed (green) time [s] Major	Minor	Signal. period [s]
20 %	100–100	12	12	30
	250–100	14	12	32
	250–250	13	13	32
	500–250	26	14	46
	750–250	55	20	81
	500–500	37	37	80
40 %	100–100	12	12	30
	250–100	15	12	33
	250–250	14	14	34
	500–250	31	16	53
	750–250	85	30	121
	500–500	57	57	120

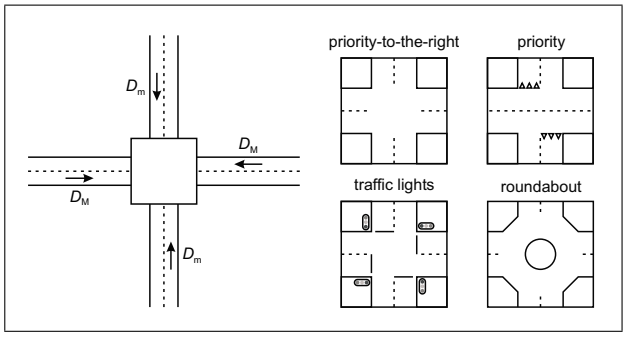

Figure 1. The four intersection types considered.

2.2. Calculation of travel times

Macroscopic traffic models often translate the effect of the presence of crossings to an additional travel time on this part of the network. Travel time is therefore a useful parameter in an engineering type correction for traffic noise emission at and immission near intersections. Calculation of travel times, averaged over 1 hour of simulation, was made on the basis of travel time data reported by Paramics, for each lane separately. The average is calculated for all trips departing within the 1-hour simulation period. This means that a number of vehicles arrive at their destination zone after the actual simulation period has ended (especially in the case of congestion). This way, the travel times can be compared to travel times generated by static assignment models, in which it is assumed that all traffic completes its journey through the network within the simulation period.

However, one has to be careful when considering travel times returned by macroscopic models. The deceleration of vehicles approaching the intersection results in an actual average speed which is lower than the free flow limit speed. In macroscopic models, this is reflected by the travel time associated with the (inbound) link of the intersection. The extra travel time associated with the intersection itself therefore only reflects possible queues and congestion. Because the travel time associated with the intersection itself (noted T) is considered in this case study, the travel times corresponding to the case where there are no queues (the zero extra intersection associated travel time situation) have to be subtracted from the travel time results obtained through microsimulation. For this, a fifth intersection type was added as a reference: a simple intersection without priority rules. Simulations of all scenarios for this reference network were divided into four parts; a separate simulation run was done for traffic originating from each arm of the network. This way, there is no interaction between vehicles of different origin zones, and vehicles reach their destination in the minimum time. The difference between the average lane travel time of the network under consideration, and the average lane travel time of the reference network then defines the average extra travel time T needed for a vehicle to cross an intersection, compared to the free flow situation where there are no delays.

It has to be noted that vehicles in this reference network still decelerate when approaching the intersection, and accelerate when leaving. Therefore this reference network can not be used as a basis for corrections on free flow noise emissions, because noise prediction models based on static traffic flows assume a constant vehicle speed on each lane. This network will only be used as a reference for travel times.

2.3. Traffic noise modeling

The noise emission of each vehicle in the simulation within a distance of 500 m from the center of the intersection, is calculated for each simulation time step using a Paramics plugin [37]. The Harmonoise road traffic noise emission model [39] is used, in which rolling noise (combined with aerodynamic noise) and propulsion (engine) noise are separately modeled. For a single vehicle, both contributions are resp. given by the following formulae:

$$L_{WR}(f) = a_R(f) + b_R(f)\log_{10}\left[\frac{v}{v_{ref}}\right], \quad (1)$$

$$L_{WP}(f) = a_P(f) + b_P(f)\left[\frac{v - v_{ref}}{v_{ref}}\right] + ca, \quad (2)$$

where v is the vehicle speed (in km·h^{-1}) with $v_{ref} = 70\,\mathrm{km\cdot h^{-1}}$, and a is the vehicle acceleration (in m·s^{-2}). For each vehicle category, the coefficients $a_X(f)$ and $b_X(f)$ are given in one-third octave bands, with center frequency f ranging from 25 Hz to 10 kHz; the coefficient c does not depend on the frequency. Only 2 types of vehicles were considered in the simulation: a default passenger car (Harmonoise emission class 1) and a truck (Harmonoise emission class 3 with 5 axles), representing the heavy traffic. The reference Harmonoise road surface was assumed (a mixture of DAC and SMA, with a chipsize of 11 mm and an age of 2 years or more).

Following the definition of the sound power level, both rolling and propulsion noise contributions are aggregated to obtain the sound power $w(f)$ of a single vehicle:

$$w(f) = W_0 \cdot \left(10^{L_{WR}(f)/10} + 10^{L_{WP}(f)/10}\right), \quad (3)$$

with $W_0 = 10^{-12}$ Watt. $w(f)$ will thus depend on the vehicle type, speed and acceleration.

The noise emission of all vehicles in a given lane segment s with length l_s during simulation is aggregated to obtain the total sound power $W_s^k(f)$ emitted by the lane segment s during the k-th timestep:

$$W_s^k(f) = \sum_{i=1}^{n_s^k} w_s^{k,i}(f), \quad (4)$$

with n_s^k the number of vehicles within the lane segment s on the k-th timestep and $w_s^{k,i}(f)$ the sound power emitted by the i-th vehicle within the lane segment s during the k-th timestep. The hourly averaged sound power $W_s(f)$ emitted by the lane segment s is then obtained by

$$W_s(f) = \frac{\Delta t}{t_{sim}} \sum_{k=1}^{t_{sim}/\Delta t} W_s^k(f), \quad (5)$$

with $t_{sim} = 3600$ s the total simulation duration and $t_{sim}/\Delta t$ the total number of timesteps in the simulation.

Finally, the hourly averaged A-weighted sound power level $L_{W,s}$ emitted by the lane segment s is given by

$$L_{W,s} = 10\log_{10}\left(\frac{\sum_f A(f) W_s(f)}{W_0}\right), \quad (6)$$

Table II. Average extra travel time T (in seconds) compared to the reference network. *Queues with impact on average noise emission are formed; **Congested lane.

Traffic demand D_M–D_m [vehicles·h^{-1}]	Priority-to-the-right		Priority		Traffic lights		Roundabout	
	Major	Minor	Major	Minor	Major	Minor	Major	Minor
100–100	3.9	3.8	0.4	3.2	8.1	8.1	1.6	1.4
250–100	6.8	5.9	0.4	4.4	8.9	8.8	1.8	1.3
250–250	24.9	22.7	0.7	7.9	10.5	9.8	2.4	2.2
500–250	408.1**	72.8*	1.2	37.6*	11.4	18.9	4.0	2.9
750–250	650.6**	93.1*	3.1	311.3**	25.7*	50.7*	8.0	4.7
500–500	559.8**	484.6**	1.5	439.5**	36.0*	38.5*	6.6	5.6

with $A(f)$ the A-weighting correction factor for the one-third octave band with center frequency f. We note that the hourly occupancy Q_s of the segment s is given by

$$Q_s = \sum_{k=1}^{t_{sim}/\Delta t} n_s^k \tag{7}$$

and is related to the traffic flow on the segment s. Traffic flow and occupancy are not equal, since vehicles standing still in the segment may be counted more than once. In free flow condition however, both are proportional quantities. Using equations (4), (5) and (7), equation (6) can be rewritten as

$$L_{W,s} = 10\log_{10}\left(\frac{\Delta t}{t_{sim}}\frac{\langle w_{A,s}\rangle}{W_0}\right) + 10\log_{10}\left(Q_s\right), \tag{8}$$

where

$$\left\langle w_{A,s}\right\rangle = \frac{1}{Q_s}\sum_f \sum_{k=1}^{t_{sim}/\Delta t}\sum_{i=1}^{n_s^k} A(f) w_s^{k,i}(f) \tag{9}$$

is the average A-weighted sound power of a single vehicle on the lane segment s.

To obtain a good spatial resolution, the segment length should be kept low. Therefore, for the calculation of the corrections in section 4 (based on $L_{W,s}$), a segment length $l_s = 5$ m was used, in which at most only one vehicle fits ($n_s^k = 0$ or 1). For the calculation of the noise maps in section 3, the noise immission level $L_{Aeq,1h}$ was calculated using the ISO 9613 propagation model [51] (hard surface), in a square area of 200 m × 200 m without buildings, departing from the hourly averaged sound power $W_s(f)$ for all lane segments.

3. Microsimulation results

3.1. Influence of scenario parameters on travel time

Table II summarizes the average extra travel time T, for both the major and minor arms of the intersection. One can see that for all networks, travel time increases with increasing traffic demand. For the major arm of the intersection, the priority junction will obviously be the best choice in all cases. For the minor arm this would be the roundabout, which also seems to be the overall best intersection layout. For low traffic demands, traffic lights have a clear disadvantage, for high traffic demands the priority-to-the-right junction is the worst choice. A t-test revealed that traffic composition F and turning rate R did not have a significant influence on travel time ($p > 0.1$); results were therefore averaged over F and R in Table II.

Some intersection scenarios resulted in congestion: no stable traffic situation was achieved on the major and/or minor inbound lanes during simulation (queue lengths grow during the full simulation due to jams). In this case the calculated travel times have high variance between different simulation runs and become unreliable. However, these types of intersections will in practice probably never be used for these traffic volumes. In some scenarios, the formation of a queue has an impact on noise emission (the effect will be quantified in section 4). Small queues can be formed in other situations, but their impact on noise emission will be negligible. E.g. for the intersection with traffic lights, at lower traffic demands still a fraction of the traffic can traverse the intersection without slowing down; the noise emission of these vehicles will then be dominant in the queuing area. Limits are not clear, but as a rule of thumb derived from Table II, one can say that important queues are formed when $T > 25$ s, and that the network is congested when $T > 100$ s.

3.2. Influence of scenario parameters on total noise emission

To have an impression of the total noise generated on the intersection, the intersection can be considered as one large emission segment. For this, the time-varying noise emission of all vehicles within a given radius from the center of the intersection was aggregated and averaged over 1 hour, using equations 4 to 6. This makes it possible to compare different scenarios using a single noise emission value. From equation 8 it can be seen that, in free flow, this sound power level increases as $10\log(Q_M + Q_m)$ since $Q_s \sim Q_M + Q_m$. Furthermore, the total noise emission also depends on the average A-weighted sound power of a single vehicle and thus on the traffic composition F. Turning rate R again was found to have no significant influence ($p > 0.1$) on total noise emission in this case study.

The resulting total noise emission will however also depend on the aggregation size. The larger the aggregation radius, the higher the total noise emission, but also the

Table III. Aggregation radius (in m) at which the difference in total noise emission between the different intersection types and the free flow situation becomes smaller than 1 dB(A).

Traffic demand D_M–D_m [vehicles·h^{-1}]	Traffic composition F 5 %	10 %	20 %
100–100	160	100	160
250–100	140	80	150
250–250	120	70	140
500–250	150	150	150
750–250	>500	>500	>500
500–500	170	120	160

smaller the differences between different types of intersections. To see this, one has to compare the four intersection types with the imaginary situation in which the two roads cross each other without any interference, and all vehicles drive with the free flow speed on the whole "intersection". This case can be seen as the absence of any influence of an intersection on the traffic flow. Differences in the noise emission between the four intersections and the imaginary free flow situation are due to the typical acceleration and deceleration profiles near intersections, the lower speeds, and to the fact that it will take a longer time to cross an actual intersection compared to the imaginary free flow "intersection". At larger distance from the center of the intersection, all vehicles will drive at the free flow speed, independent of the type of intersection.

It is interesting to look at the aggregation radius needed to make the difference in total noise emission between the different intersection types and the free flow situation smaller than 1 dB(A). Table III shows that this radius varies between 70 and 170 m for the non-congested scenarios (corresponding to a segment length of 140 to 340 m). When noise maps are drawn with this resolution, one can have 1 dB(A) accuracy on average noise exposure, without having to bother about intersection corrections. The aggregation radius needed for this accuracy is smallest for intermediate traffic demands and a percentage of heavy vehicles of 10 %. In the case of heavy congestion, it was found that 1 dB(A) accuracy could not be achieved with an aggragation radius smaller than 500 m.

3.3. Influence of scenario parameters on noise immission

As an example, Figure 2 shows a noise map of the signalized intersection, together with the differences in noise immission level with the other 3 types of intersections considered. As can be seen, the intersection type has a large influence on vehicle speed and acceleration, and as a consequence on local noise immission. Differences in local $L_{Aeq,1h}$ can be up to 2 to 3 dB(A) with the priority-to-the-right and priority intersection. The noise map of the priority intersection seems to reproduce the results found in [42] and discussed in the introduction; however, only for the priority arm. The large differences for the roundabout can be attributed to the different physical road layout and to the higher average speeds of approaching traffic on signalized intersections. At some distance from the center, a reduction of several dB(A) is found for the roundabout compared with the signalized intersection, which is in agreement with earlier measurements [40]. For the priority junction, noise emission is larger along the major road because vehicles do not have to slow down, but smaller near the stoplines and on the minor road where all vehicles slow down or stop. For the priority-to-the-right junction, the opposite is true: the highly interrupted traffic results in slightly higher noise levels near the center and stoplines of the intersection, but lower levels at some distance. From this, it can be concluded that noise emission corrections should be made spatially dependent. These conclusions remain quantitatively valid for all non-congested scenarios considered.

So far, only the energetic mean of the results of the 5 simulation runs was presented. In Figure 3, the standard deviation of the 5 simulation runs that led to the maps in Figure 2 are shown. The small dots appearing along the lanes are related to the discretization involved in microsimulation models. The largest modeling uncertainty can be found at the locations where the traffic is most interrupted, and where small jams are formed, mostly on the minor arms of the intersection. There may be two explanations for this. Firstly, the dependence on acceleration behaviour and corresponding increase in sound levels is larger in these areas. Secondly, and probably more importantly, the length of the queue waiting to enter the intersection is very chaotic and unpredictable, also on real junctions with approximately this traffic load. Thus, provided that the number of simulations leading to the average effect is large enough, corrections for these types of intersections could still be extracted from the simulations, but they will certainly not be valid for comparison to short term observations. Further away from the road, the standard deviation is smaller than 0.5 dB(A), thus leading to errors well below 1 dB(A) on proposed intersection corrections. This does not exclude the possibility that other, systematic errors exist, but it is at least a good indication.

4. Emission corrections

In this section, an onset is given in formulating corrections, which can be applied to the noise emission obtained through the use of macroscopic traffic models that do not take into account traffic dynamics on intersections. As already mentioned in the previous section, some intersection scenarios resulted in a congested major and/or minor inbound lane; these lanes are excluded from the correction analysis. The outbound lanes of these configurations were nevertheless taken into account, since no jams are formed there. The roundabout is not taken into account for the correction analysis, as the layout of this type of intersection differs highly from the other 3 types.

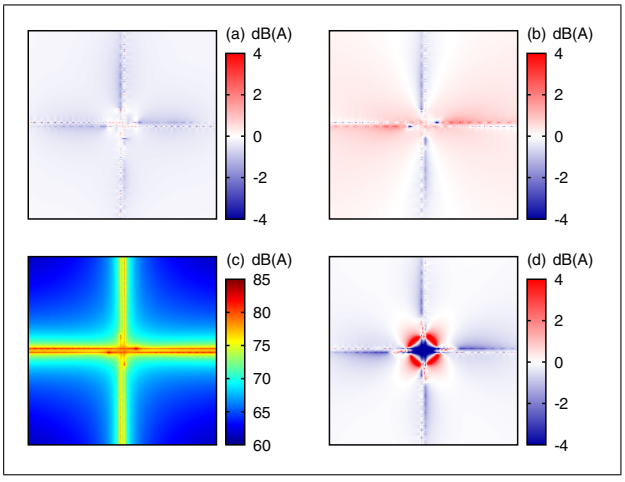

Figure 2. Noise maps ($L_{Aeq,1h}$) of (a) the difference between the priority-to-the-right and the signalized intersection, (b) the difference between the priority and the signalized intersection, (c) the signalized intersection and (d) the difference between the roundabout and the signalized intersection (D_M = 250 vehicles·h^{-1}, D_m = 100 vehicles·h^{-1}, F = 20 %, R = 20 %).

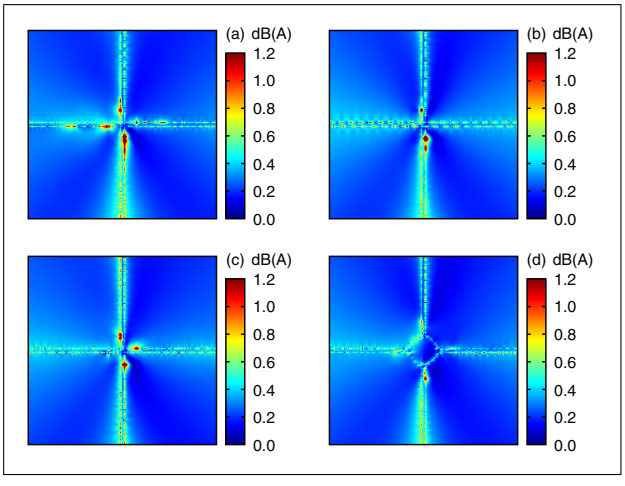

Figure 3. Maps of the standard deviation in noise immission level ($L_{Aeq,1h}$), calculated over 5 simulation runs with different seed values, for (a) the priority-to-the-right, (b) the priority and (c) the signalized intersection, and (d) the roundabout (D_M = 250 vehicles·h^{-1}, D_m = 100 vehicles·h^{-1}, F = 20 %, R = 20 %).

4.1. Noise emission profile

It is assumed that the noise emission, obtained through the use of macroscopic traffic modeling, consists of a series of static sound sources with hourly averaged A-weighted sound power level $L_{W,s}$ (equation 6), associated to segments of a lane of the road. Figure 4 shows an example of a simulated noise emission profile $L_{W,s}$ along a lane of the intersection; the other scenarios produce similar profiles. A segment length of 5 m was used, as explained in section 2.3. A larger segment length would obfuscate the fine structure of local noise emission near the center of the intersection, while a smaller segment length would not give additional information, since at most 1 vehicle can be in each segment at any time. One could subtract

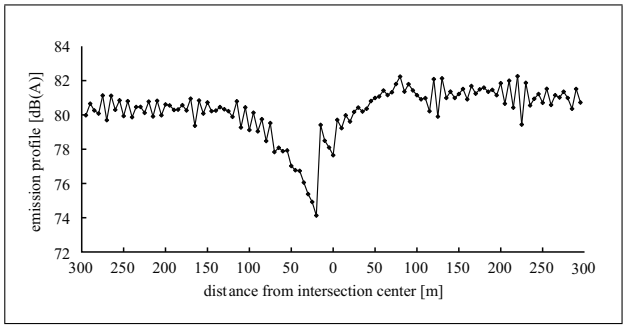

Figure 4. Noise emission profile $L_{W,s}$ for the inbound (left) and outbound (right) lane of the major arm of the priority-to-the-right intersection (D_M = D_m = 100 vehicles·h^{-1}, F = 5 %, R = 40 %), averaged over 5 simulation runs.

$10\log_{10}(5) \approx 7$ dB(A) to get the noise emission per lane in segments of 1 m length; this has however no implications for the derivation of the correction factors, as only differences in sound power level will be considered.

At larger distances from the junction the noise emission is independent of the location, as can be expected for cruising vehicles. The hourly averaged A-weighted sound power level emitted by a segment s at large distance from the junction will be referred to as $\widetilde{L}_{W,s}$. The corresponding value of the average A-weighted sound power of a single vehicle cruising at large distance from the junction is $\langle \tilde{w}_A \rangle$. Noise corrections will be based on the limit value $\widetilde{L}_{W,s}$, as it is assumed that this is the usual emission output of traffic noise prediction based on a macroscopic model. Closer to the intersection (which is at the origin in Figure 4), different regions can be observed.

On the inbound lane, the noise emission starts to drop at some distance from the intersection, as vehicles start to decelerate. Just before the intersection (at the stopline), a small discontinuous peak is observed, due to the high engine speed and associated acceleration of departing vehicles, which is accounted for in the propulsion contribution (equation 2). Beyond the stopline, the average noise emission decreases as the acceleration decreases. When a significant queue is formed on the inbound lane, the vehicle acceleration peak is spread out in a larger area before the stopline, which we will call the queuing zone. On the outbound lane the sound level rises to the cruising value over a limited distance, due to the increasing average vehicle speed.

4.2. General methodology

In a segment s near the intersection, the variability of the vehicle speed and acceleration changes the average A-weighted sound power of a single vehicle. This can be represented by a correction factor C_s:

$$\langle w_{A,s} \rangle = \langle \tilde{w}_A \rangle C_s. \tag{10}$$

According to equation (8), this is equal to applying a correction term on the hourly averaged A-weighted sound power level emitted by the segment s:

$$L_{W,s} = \widetilde{L}_{W,s} + 10\log_{10}\left(C_s\right). \tag{11}$$

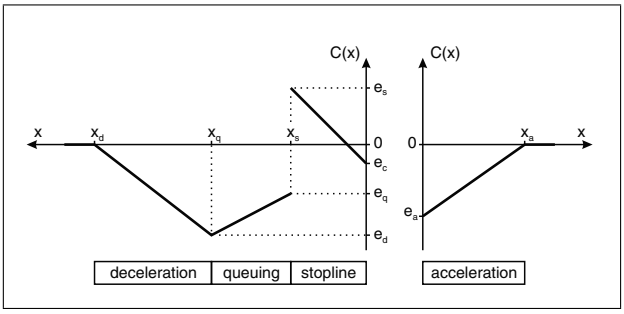

Figure 5. Proposed inbound (left) and outbound (right) correction function for the priority-to-the-right, priority and signalized intersections.

The correction factor C_s may be evaluated as the average of a correction function $C(x)$ over the length of the segment s:

$$C_s = \frac{1}{l_s}\int_s 10^{C(x)/10}\mathrm{d}x. \quad (12)$$

The correction function $C(x)$ is estimated by the simulated noise emission profiles. According to Figure 4, a piecewise linear function of the distance x to the center of the junction seems suitable. Based on the above findings, and inspired by previous work in the field of particle emissions [52, 53] by vehicles near intersections, a spatial approach will be used, in which inbound and outbound lanes are divided into deceleration, queuing, stopline and acceleration zones. The proposed model for the correction function $C(x)$ is shown in Figure 5. For example, for the deceleration area, one has

$$C(x) = e_d - e_d\frac{x - x_q}{x_d - x_q} \quad \text{for} \quad x_q < x \leq x_d. \quad (13)$$

Vehicles approaching the intersection will on average start decelerating at a distance x_d from the center of the intersection. This is modeled by a decrease in noise emission proportionally to the distance x, up to a distance x_q where a possible queue starts. The noise emission is again linearly modeled in this queuing zone. At the distance x_s on the inbound road, the vehicles start accelerating, which results in a peak in the noise emission near the stopline of the inbound lane ($x_s = 12.5$ m in this study). On the outbound lane, the acceleration noise emission is also modeled as a linear function of the distance x, up to a distance x_a from the intersection, where the outbound lane free flow speed is reached. The emission values e_d, e_q, e_s, e_c and e_a represent the increase (or decrease if negative) in hourly averaged A-weighted sound power level, compared to the limit emission value (inbound or outbound).

The curve $C(x)$ was fitted to the noise emission profiles of all intersection scenarios considered, using a least squares method. The standard deviation of the fitted model error varied from 0.2 to 1.7 dB(A) for the different scenarios, with a mean of 0.6 dB(A). Meaningful relationships between the traffic flow parameters (Q_x, F, R, T) and the correction model parameters (x_i, e_j) were then derived by the use of standard linear regression analysis; for each linear regression model, parameters that did not pass a t-test ($\alpha = 0.05$) were excluded from the analysis. It was found that the best correlation could be achieved when $\log_{10} Q_x$ and $\log_{10} T$ are used instead of Q_x and T. It has to be noted that the given formulas are only valid within the simulated limits, which are from 5 % to 20 % for F, from 100 to 750 vehicles·h^{-1} for Q (subscripts are dropped from here on), from 20 % to 40 % for R, and roughly between 0.1 s and 100 s for T. Extrapolations outside these intervals should be handled with caution.

All correction factors given are for a single lane road with a limit speed of 70 km·h^{-1}. In the case of multiple lanes, the corrections can be applied to each lane separately, provided that traffic intensity and composition is known for each lane, as well as the turning rate. A reduction of the speed limit to 50 km·h^{-1} will however require additional simulations, since this has a large impact on free flow emissions, as well as on traffic dynamics, such as the formation of queues.

4.3. Regression analysis results

Table IV summarizes the results for the deceleration zone. For the major arm of the priority network, no corrections are found, because the larger part of the vehicles does not accelerate nor decelerate on this arm; traffic on this arm has priority. No significant difference was found between the major and the minor arms of the priority-to-the-right and the signalized intersections. A positive correlation with the extra travel time $\log_{10} T$ and/or the traffic intensity $\log_{10} Q$ was found for x_d as well as for e_d. E.g. for the priority-to-the-right intersection, the following relationships were found:

$$x_d = 167.8 \log_{10} T, \quad (14)$$

$$e_d = -9.8 + 5.4 \log_{10} T. \quad (15)$$

In this case, the longer the delay or the queue at the intersection, the larger the distance at which a correction should be applied, but the less the actual reduction in sound emission. Obviously T has to be >1 s to result in a positive x_d; however, T was found to be at least 3 s in the priority-to-the-right intersection.

For the queuing area, no significant differences were found between the different types of intersections, but a classification based on the extra travel time was made; correction coefficients are shown in Table V. A queuing area only exists when $\log_{10} T > 1.4$, as already mentioned in section 3.1; otherwise x_q can be chosen at the stopline x_s. Only $\log_{10} T$ was found to be a significant predictor for the queuing area correction. The fraction of heavy vehicles F (in %) also had some influence on x_q (heavy vehicles are also longer), but this was not statistically significant ($p = 0.066$).

Noise emission corrections at the stopline (e_s) are mainly influenced by the extra travel time associated with the inbound arm and by the fraction of heavy vehicles, as summarized in Table VI. The correction starts slightly negative for low values of T and F. A larger average extra

Table IV. Correction coefficients for the deceleration area; t-values are given between brackets. $^{*}p < 0.05$, $^{**}p < 0.01$, $^{***}p < 0.001$.

x_d [m]	Priority-to-the-right	Priority		Traffic lights
		Major	Minor	
r^2	0.89	-	0.90	0.80
constant		0.0		-254.7 (-8.1***)
$\log_{10} Q$				96.9 (6.7***)
$\log_{10} T$	167.8 (55.9***)		164.5 (37.6***)	200.5 (6.7***)
e_d [dB(A)]	Priority-to-the-right	Priority		Traffic lights
		Major	Minor	
r^2	0.82	-	0.97	0.73
constant	-9.8 (-23.5***)	0.0	-10.6 (-55.5***)	-8.8 (-20.2***)
$\log_{10} Q$				2.5 (13.8***)
$\log_{10} T$	5.4 (12.5***)		5.6 (28.7***)	

Table V. Correction coefficients for the queuing area; t-values are given between brackets. $^{*}p < 0.05$, $^{**}p < 0.01$, $^{***}p < 0.001$.

x_q [m]	All intersection types	
	$\log_{10} T < 1.4$	$\log_{10} T > 1.4$
r^2	-	0.51
constant	x_s	-81.5 (-2.7**)
$\log_{10} T$		116.4 (6.4***)
e_q [dB(A)]	All intersection types	
	$\log_{10} T < 1.4$	$\log_{10} T > 1.4$
r^2	-	0.73
constant	0.0	-8.2 (-8.9***)
$\log_{10} T$		5.8 (10.4***)

travel time is caused by vehicles slowing down when arriving at the intersection. The subsequent acceleration near the stopline then results in a higher e_s, which can eventually rise to 7 dB(A) for high traffic intensities. As can be expected, the correction is smaller for the signalized intersection, because a large part of the traffic here can cross the intersection without stopping. Again, no correction is found for the major priority arms of priority junctions.

For the priority-to-the-right intersection, it was found that the corrections at the center (e_c) could best be described by a subdivision based on $\log_{10} T$, analogous to the queuing correction; for higher T the correction becomes smaller. A small center correction e_c for the major arm of the priority network was found, mainly correlated to the percentage R of traffic turning left or right.

Finally, results for the acceleration area are given in Table VII. For all intersection types, the amount of heavy traffic has the largest influence on the length x_a of the acceleration area, because the maximum acceleration for heavy traffic is lower. For the priority-to-the-right junction, it is found that also the traffic volume makes the acceleration after a junction more slowly; vehicles are more interrupted at the crossing when the traffic volume increases. Note that the traffic volume on the outbound lane is influenced by both the traffic volume on the minor and the major inbound arms. On the minor outbound arm of the priority junction, the length of the acceleration area is to a small extent also influenced by the amount of vehicles that enters this lane from the major arm (turning rate R). For the signalized intersection, the influence of the heavy traffic percentage becomes smaller, because during the green-time on the major arm (which is most of the time), vehicles do not have to decelerate at the crossing. No significant correlations were found for e_a, but the variations in this coefficient were small, so the average is given in Table VII. In all cases, a negative e_a was found; positive values (corresponing to higher levels due to acceleration) may be possible if the speed limit on the outbound lane is lower.

5. Discussion and conclusions

Current traffic noise prediction models, which are mostly based on macroscopic traffic simulation, do not allow to study the influence of traffic dynamics near junctions on local noise levels. The goal of this research was to prove that it is possible to refine noise calculations based on the output of these models in the neighbourhood of intersections, using a correction on the average vehicle emission, aggregated in lane segments. For this, a case study consisting of the microsimulation of a large set of intersection scenarios was conducted. The intersection type was found to have a significant influence on travel times. Global noise emission of the different intersection types was compared to the situation in which the presence of an intersection is neglected when calculating noise emissions. It was found that, in the non-congested state, the variation in total noise emission between different intersection types becomes lower than 1 dB(A) when one aggregates over segments with a length of 140 to 340 m, depending on the traffic demand and composition. Noise immission calculations for the intersection scenarios were compared to some previous measurement results found in literature, and in general a good agreement was found.

However, there were large spatial differences in noise emission. The results indicated that a spatial approach should be used; deceleration, queuing, stopline and accel-

Table VI. Correction coefficients for the stopline area; t-values are given between brackets. $^{*}p < 0.05$, $^{**}p < 0.01$, $^{***}p < 0.001$.

x_d [m]	Priority-to-the-right	Priority		Traffic lights
		Major	Minor	
r^2	0.90	-	0.91	0.53
constant	-3.1 (-9.0***)	0.0	-3.4 (-9.5***)	-1.8 (-3.5***)
$\log_{10} T$	4.3 (19.7***)		5.3 (14.5***)	3.2 (8.0***)
F	0.06 (3.1**)			0.06 (3.0**)

e_c [dB(A)]	Priority-to-the-right		Priority		Traffic lights	
	$\log_{10} T < 1.4$	$\log_{10} T > 1.4$	Major	Minor	Major	Minor
r^2	0.60	0.50	0.73	0.66	0.64	0.41
constant	12.0 (5.3***)	-5.5 (-6.7***)	1.8 (2.7*)	10.0 (5.6***)	-4.8 (-15.4***)	-3.4 (-9.5***)
$\log_{10} Q$	-7.7 (-5.9***)		-0.73 (-3.0**)	-5.1 (-5.7***)		
$\log_{10} T$	2.7 (2.8**)	1.7 (3.7**)		1.6 (3.9***)	2.1 (7.7***)	1.4 (4.8***)
R			-0.06 (-8.9***)	-0.04 (-3.7**)		

Table VII. Correction coefficients for the acceleration area; t-values are given between brackets. For e_a, the average and standard deviation are given. $^{*}p < 0.05$, $^{**}p < 0.01$, $^{***}p < 0.001$.

x_a [m]	Priority-to-the-right	Priority		Traffic lights
		Major	Minor	
r^2	0.81	-	0.50	0.65
constant	-35.0 (-3.5***)	0.0	47.1 (6.2***)	33.7 (27.3***)
$\log_{10} Q$	33.5 (8.1***)			
F	2.0 (15.8***)		1.8 (5.2***)	1.0 (11.3***)
R			-0.54 (-2.6*)	

e_a [dB(A)]	Priority-to-the-right	Priority		Traffic lights
		Major	Minor	
constant	-1.81 ± 0.20	0.0	-2.28 ± 0.61	-2.41 ± 0.42

eration zones were observed. A correction model, based on a piecewise linear approximation of the average noise emission by all vehicles in each lane segment close to the intersection, was proposed. Finally, it was shown that meaningful relationships can be derived between the proposed noise emission corrections and traffic flow parameters. The results obtained in this paper are only applicable for the range of traffic situations studied. The methodology can however easily be used to study typical intersections for a region and to extrapolate the results to the whole network under study.

Acknowledgments

This research was conducted in the framework of the IMAGINE project [48], funded by the Sixth Framework Programme of the European Community. The authors wish to thank all people in the Work Package 2 group for the animated discussions and their many useful comments. Furthermore, the authors wish to thank the reviewers for their valuable suggestions.

References

[1] C. Steele: A critical review of some traffic noise prediction models. Applied Acoustics **62** (2001) 271–287.

[2] J. J. A. van Leeuwen, D. Manvell, R. Nota: Some prediction models for the calculation of traffic noise in the environment. Proceedings of The 25th International Congress on Noise Control Engineering (Inter·noise), Liverpool, UK, Juli 1996.

[3] Guide du bruit des transports terrestres — Prévision des niveaux sonores (a guide to land transportation noise impacts — Prediction of sound levels). Centre d'Étude des Transports Urbain (CETUR), Nov. 1980.

[4] Bruit des infrastructures routières — Méthode de calcul incluant les effets météorologiques NMPB-96 (noise related to road infrastructure projects — New French calculation method including meteorological effects NMPB-96). CERTU, Jan. 1997.

[5] CRTN — Calculation of road traffic noise. Department of Transport, Welsh Office, London, 1988.

[6] K. Heutschi: SonRoad: New Swiss road traffic noise model. Acta Acustica united with Acustica **90** (2004) 548–554.

[7] F. Besnard, J. Lelong, S. Doisy, V. Steimer: Updating the vehicle noise emission values used in French traffic noise prediction models. Proceedings of The 28th International Congress on Noise Control Engineering (Inter·noise), Fort Lauderdale, Florida, USA, Dez. 1999.

[8] J. Kragh, B. Plovsing, S. A. Storeheier, G. Taraldsen, H. G. Jonasson: Nordic environmental noise prediction methods, Nord2000. summary report. General Nordic sound propagation model and applications in source-related prediction methods. Tech. Rept. AV 1719/01, DELTA Acoustics & Vibration, Lyngby, 2001.

[9] H. G. Jonasson, S. A. Storeheier: Nord 2000. New Nordic prediction method for road traffic noise. Tech. Rept. 2001:10, SP Swedish National Testing and Research Institute, Borås, 2001.

[10] RMW2002 — Reken- en meetvoorschrift wegverkeerslawaai. Ministry of Housing, Spatial Planning and the Environment (VROM), Staatscourant 62, März 2002. http://www.stillerverkeer.nl.

[11] RLS90. Richtlinien für den Lärmschutz an Strassen. BM für Verkehr, Bonn, 1990.

[12] C. W. Menge, C. F. Rossano, G. S. Anderson, C. J. Bajdek: FHWA traffic noise model. Tech. Rept. FHWA-PD-96-010, U.S. Department of Transportation, Federal Highway Administration, 1996.

[13] H. Tachibana, K. Yamamoto, S. Kono, Y. Oshino, T. Iwase, T. Sone, K. Yoshihisa, T. Miyake, T. Tajika: Road traffic noise prediction model "ASJ RTN-Model 2003" proposed by the Acoustical Society of Japan. Proceedings of The 18th International Congress on Acoustics (ICA), Kyoto, Japan, Apr. 2004.

[14] K. Yoshihisa, Y. Oshino, K. Yamamoto, H. Tachibana: Road traffic noise prediction in the vicinity of signalized intersections in urban areas. Proceedings of The 18th International Congress on Acoustics (ICA), Kyoto, Japan, Apr. 2004.

[15] V. Desarnaulds, G. Monay, A. Carvalho: Noise reduction by urban traffic management. Proceedings of The 18th International Congress on Acoustics (ICA), Kyoto, Japan, Apr. 2004.

[16] D. Gilbert: Noise from road traffic (interrupted flow). J. Sound. Vib. **51** (1977) 171–181.

[17] P. T. Lewis, A. James: On the noise emitted by single vehicles at roundabouts. J. Sound. Vib. **58** (1978) 293–299.

[18] P. T. Lewis, A. James: Noise levels in the vicinity of traffic roundabouts. J. Sound. Vib. **72** (1980) 51–69.

[19] I. S. Diggory, B. Oakes: Computer simulation model for the prediction of traffic noise levels. Applied Acoustics **13** (1980) 19–31.

[20] R. R. K. Jones, D. C. Hothersall, R. J. Salter: Techniques for the investigation of road traffic noise in regions of restricted flow by the use of digital computer simulation methods. J. Sound. Vib. **75** (1981) 307–322.

[21] K. S. Jraiw: A computer model to assess and predict road transport noise in built-up areas. Applied Acoustics **21** (1987) 147–162.

[22] M. M. Radwan, D. J. Oldham: The prediction of noise from urban traffic under interrupted flow conditions. Applied Acoustics **21** (1987) 163–185.

[23] B. Favre: Noise at the approach to traffic lights: Result of a simulation programme. J. Sound. Vib. **58** (1978) 563–578.

[24] L. J. M. Jacobs, L. Nijs, J. J. van Willigenburg: A computer model to predict traffic noise in urban situations under free flow and traffic light conditions. J. Sound. Vib. **72** (1980) 523–537.

[25] L. Nijs: The increase and decrease of traffic noise levels at intersections measured with a moving microphone. J. Sound. Vib. **131** (1989) 127–141.

[26] J. Lelong, L. Leclercq: Steps towards a better evaluation of urban traffic noise. Proceedings of The 6th International Congress on Sound and Vibration (ICSV), Lyngby, Copenhagen, Denmark, Juli 1999.

[27] L. Leclercq, J. Lelong: Dynamic evaluation of urban traffic noise. Proceedings of The 17th International Congress on Acoustics (ICA), Rome, Italy, Sep. 2001.

[28] L. Leclercq, J. Lelong, J. Defrance: Dynamic assessment of road traffic noise: elaboration of a global model. Proceedings of The 18th International Congress on Acoustics (ICA), Kyoto, Japan, Apr. 2004.

[29] Y. Oshino, H. Tachibana: Prediction of road traffic noise taking into account of transient running conditions of vehicles. Proceedings of The 22nd International Congress on Noise Control Engineering (Inter·noise), Leuven, Belgium, Aug. 1993.

[30] Y. Oshino, K. Tsukui, H. Tachibana: Road traffic noise prediction taking account of transient vehicle running conditions. Proceedings of The 25th International Congress on Noise Control Engineering (Inter·noise), Liverpool, UK, Juli 1996.

[31] T. Suzuki, K. Tsukui, Y. Oshino: Road traffic noise prediction model around signalized intersections. Proceedings of The 32nd International Congress on Noise Control Engineering (Inter·noise), Jeju Island, South Korea, Aug. 2003.

[32] J. L. Parrondo, F. Fernández, J. Fernández, J. González, S. Velarde: Prediction of noise indexes in urban streets with fluctuating vehicle traffic, based on the acoustic ray method. Proceedings of The 6th International Congress on Sound and Vibration (ICSV), Lyngby, Copenhagen, Denmark, Juli 1999.

[33] R. Zurita, J. Parrondo, O. Díaz, J. A. Corrales: Numerical simulation of the noise distribution due to vehicle traffic in intersections of urban streets. Proceedings of The 12th International Congress on Sound and Vibration (ICSV), Lisbon, Portugal, Juli 2005.

[34] R. Liu, D. Van Vliet, D. P. Watling: DRACULA: Dynamic route assignment combining user learning and microsimulation. Proceedings of the 23rd PTRC European Transport Forum, Warwick, UK, Sep. 1995, 143–152.

[35] P. S. Goodman, M. C. Bell, N. Hodges: The AVTUNE Noise Model. Proceedings of the 11th International Symposium on Transport and Air Pollution, Graz, Austria, Juni 2002.

[36] P. S. Goodman, M. C. Bell: Validation of the TUNE microscopic traffic noise model. Proceedings of the 35th Annual Universities' Transport Study Group Conference (UTSG), Loughborough, UK, Jan. 2003.

[37] B. De Coensel, T. De Muer, I. Yperman, D. Botteldooren: The influence of traffic flow dynamics on urban soundscapes. Applied Acoustics **66** (2005) 175–194.

[38] D. Botteldooren, B. De Coensel, T. De Muer: The effect of traffic flows on urban soundscape dynamics and how to analyze it. Proceedings of The 18th International Congress on Acoustics (ICA), Kyoto, Japan, Apr. 2004.

[39] H. Jonasson, U. Sandberg, G. van Blokland, J. Ejsmont, G. Watts, M. Luminari: Source modelling of road vehicles. Technical Report — Deliverable 9 of the Harmonoise project HAR11TR-041210-SP10, Dez. 2004.

[40] M. Bérengier: Acoustical impact of traffic flowing equipments in urban area. Proceedings of Forum Acusticum, Sevilla, Spain, Sep. 2002.

[41] J. Picaut, M. Bérengier, E. Rousseau: Noise impact modelling of a roundabout. Proceedings of The 2005 Congress and Exposition on Noise Control Engineering (Inter·noise), Rio de Janeiro, Brazil, Aug. 2005.

[42] M. A. Sattler: Assessment of noise impact determined by binary traffic systems. Proceedings of Forum Acusticum, Berlin, Germany, März 1999.

[43] W. M. To, T. M. Chan: The noise emitted from vehicles at roundabouts. J. Acoust. Soc. Am. **107** (2000) 2760–2763.

[44] P. Kokowski, R. Makarewicz: Interrupted traffic noise. J. Acoust. Soc. Am. **101** (1997) 360–371.

[45] R. Makarewicz, M. Fujimoto, P. Kokowski: A model of interrupted road traffic noise. Applied Acoustics **57** (1999) 129–137.

[46] P. Kokowski: Interrupted traffic noise at signalised intersections. Proceedings of The 6th International Congress on Sound and Vibration (ICSV), Lyngby, Copenhagen, Denmark, Juli 1999.

[47] R. Makarewicz: Noise from a road intersection. Acta Acustica united with Acustica **89** (2003) 844–847.

[48] See http://www.imagine-project.org.

[49] Highway Capacity Manual 2000. Transportation Research Board, National Research Council, Washington D.C., USA, 2000.

[50] http://www.paramics-online.com. Paramics is being developed by Quadstone Ltd.

[51] Acoustics — Attenuation of sound during propagation outdoors — Part 2: General method of calculation. International Standard ISO 9613-2, International Organization for Standardization, Geneva, Switzerland, Dez. 1996.

[52] J. W. D. Boddy, R. J. Smalley, P. S. Goodman, J. E. Tate, M. C. Bell, A. S. Tomlin: The spatial variability in concentrations of a traffic-related pollutant in two street canyons in York, UK — Part II: The influence of traffic characteristics. Atmospheric Environment **39** (2005) 3163–3176.

[53] J. Tate, M. Bell, R. Liu: The application of an integrated traffic microsimulation and instantaneous emission model to study the temporal and spatial variations in vehicular emissions at the local-scale. Proceedings of the 14th International Symposium on Transport and Air Pollution, Graz, Austria, Juni 2005.